Study of the Impact of Loads on the Deformation of Building Structures using Differential Equations

MARYNA BELOVA, VOLODYMYR DENYSENKO, SVITLANA KARTASHOVA,
VALERIJ KOTLYAR, STANISLAV MIKHAILENKO
Department of Digital Economy and System Analysis,
State University of Trade and Economics,
19 Kyoto Str., Kyiv, 02156
UKRAINE

Abstract: - The paper investigates the influence of different types of loads on the deformation of building structures, particularly beams, using second-order differential equations that allow modeling deformation processes. For this purpose, we considered two beam deflection equations under concentrated and distributed loads. Several experiments were conducted under different geometrical conditions (variable parameters of the beam cross-section, length, and loads). The solutions were studied using graph-analytical methods: constructing a graph of solutions reflecting the system's behaviour, a hodograph allowing tracking of additional nuances of the studied process, and amplitude and phase-frequency characteristics. The influence of conditions on the nature of system behavior is determined. The study's results can be used to optimise design solutions in construction.

Key-Words: - differential equations, beam deflection, hodograph, amplitude phase-frequency characteristic, second-order curves, building structures.

Received: April 25, 2024. Revised: October 26, 2024. Accepted: November 27, 2024. Published: December 31, 2024.

1 Introduction

In the construction industry, modeling and careful analysis of the behaviour of structures under various types of loads is an important step. This is necessary to ensure the reliability of construction projects in operation. To study the effect of concentrated and distributed loads on the deformation of structures, in particular beams, it is advisable to use second-order differential equations [1], which allow for detailed analysis and modelling of the behaviour of structures. The analysis of their solutions is particularly relevant, as it makes it possible to:

- understand how the system functions and what physical or mathematical laws govern its behaviour. This, in turn, allows us to predict and control the behaviour of the system;
- determine such properties of the system as stability, convergence, extremes, periodicity and other characteristics;
- to assess the adequacy of the results obtained to verify the realism of the model and its compliance with experimental data;
- to identify new phenomena or patterns that may be useful for further study and development of science and technology, [2].

Second-order differential equations play an essential role in physics, engineering, and other scientific disciplines due to their ability to model various physical phenomena. However, they can be challenging to solve due to several features: nonlinearity, lack of analytical solutions, presence of derivatives with negative values, the need to define boundary conditions, etc.

The study aims to study the influence of various types of loads on building structures using second-order differential equations.

Objectives of the study:

- selection of two second-order equations (beam deflection equations with concentrated and distributed load).
- checking the stability of the selected equations;
- solving these equations for different geometric conditions;
- plotting solutions for each load condition to visualize and compare them;
- building hodographs to detect amplitudes and phase shifts in solutions;
- analysis of the results.

2 Literature Review

Many scientific papers have studied differential equations and their solutions over the years. For example, authors in [3] determined whether a sequence of minimizers converges to the solution of partial differential equations. To achieve this goal, they used neural networks and Schauder's Approach.

Other authors in [4] investigating the spring-pendulum obtained the system's equations of motion using the Lagrange and Hamilton equations. Paper [5] aims to study the geometry and physics of the Raychaudhuri equation in the homogeneous and anisotropic spacetime described by the Kantowski-Sachs metric. Authors in [6] improved Hille-type oscillation conditions for quasilinear functional dynamical equations of the second order with arbitrary time were developed. The authors argue that these findings extend and enhance previous studies. Paper [7] is devoted to the heat conduction equation, a parabolic partial differential equation characterising the diffusion process. The authors consider a new fractional operator based on the Rabotnov fractional-exponential kernel. The authors in [8] study three models where the kernels are a power law, an exponential decay law, and a generalised Mittag-Leffler kernel law. A detailed analysis is presented for each case, including numerical solution, stability analysis, and error analysis. Article [9] is devoted to positive solutions and stability of Atangana-Baleanu-Caputo fractional differential equations with singularity and nonlinear p - Laplacian. A similar study was conducted [10], which analyzed the stability of neutral stochastic differential equations and established the existence of solutions and stability for impulsive neutral stochastic equations. The authors in [11] conducted the stability analysis and proposed a numerical algorithm to study the fractional vibration equation. Article [12] presents a new bilinear neural network method and proposes a corresponding tensor formula for obtaining accurate analytical solutions to nonlinear partial differential equations.

Nevertheless, researchers have paid little attention to the solutions of differential equations, which could provide more helpful information about the processes they model.

3 Methods

This paper focuses on two second-order differential equations: the beam deflection equation under concentrated load (1) and beam deflection under distributed load (2).

For the deflection v(x) of a beam under the action of a concentrated moment, the second-order differential equation is as follows:

$$\frac{d^2}{dx^2}(EI\frac{d^2v}{dx^2}) = M_0\delta(x-a); \tag{1}$$

where v(x) is the beam deflection at distance x;

M_0 is the concentrated moment applied to the beam;

E is the Young's modulus of the beam material;

I am the moment of inertia of the beam cross-section, calculated by the width b and the height of its cross-section h:

$$I = \frac{bh^3}{12}. \tag{2}$$

δ(x - a) – is the Dirac's delta function, indicating that the moment M_0 is applied at the point x = a (in the models constructed in this study, the concentrated moment is applied to the geometric center of the beam to simplify the simulation).

The second-order differential equation for the deflection of a beam under a distributed is as follows:

$$\frac{d^2v}{dx^2} = \frac{q}{2EI}(x-a)^2(l-x); \tag{3}$$

where $v(x)$ is the beam deflection at distance x;

$q(x)$ is a function of the distributed load along the length of the beam;

a - load position on the beam;

l is the length of the beam.

Before studying the solutions of these equations and the influence of geometric conditions on them, it is advisable to confirm or refute the hypothesis of their stability. A differential equation's stability is its property of preserving the nature of solutions regardless of the initial conditions. A differential equation is usually considered stable if small changes in the initial conditions or input signals do not lead to significant changes in the system's solution over time.

In this paper, the Routh-Hurwitz stability criterion determines the asymptotic stability of the studied equations. The algorithm for its determination is as follows:

1. Find a characteristic polynomial that has the following general form:

$$\lambda(x) = a_0x^n + a_1x^{n-1} + ... + a_n. \tag{4}$$

2. The coefficients of the characteristic polynomial are used to create the Hurwitz determinant n using an algorithm:

1) all the coefficients of the characteristic polynomial from a_1 to a_0 are placed from left to right along the main diagonal;

2) from each element of the diagonal, fill in the columns of the determinant in the up and down directions so that the indices decrease from top to bottom;

3) Zeros are placed in the case of coefficients with indices less than zero or greater than n.

Then, according to the Hurwitz criterion, [13]:

For a dynamical system to be stable, all diagonal minors of the Hurwitz determinant must be positive.

Consider the beam deflection equation with a concentrated moment (1). Its characteristic polynomial corresponds to the equation of the substituted wave operator. For this equation, where there are no higher-order derivatives, the characteristic polynomial has degree 2 and is equal to 0:

$$\lambda^2 = 0; \quad a^0 = 0,\ a_1 = 0,\ a_2 = 1. \tag{5}$$

Then, the Routh-Hurwitz matrix has the following form:

$$\begin{bmatrix} a_2 & a_0 \\ a_1 & 0 \end{bmatrix} = \begin{bmatrix} 1 & 0 \\ 0 & 0 \end{bmatrix}; \tag{6}$$

Accordingly, the primary minor determinant is equal:

$$\Delta_1 = a_2 = 1; \quad \Delta_2 = \begin{vmatrix} a_2 & a_0 \\ a_1 & 0 \end{vmatrix} = a_2 \cdot 0 - a_0 \cdot a_1 = 0. \tag{7}$$

This system is stable since all minor determinants are nonnegative numbers $\Delta_1=1>0$, $\Delta_2=0\geq 0$.

Similarly, let us test the hypothesis of stability of the beam deflection equation under the distributed load (2):

Its characteristic polynomial has degree 4 and is equal to 0:

$$\lambda^4 = 0; \quad a^0 = 0,\ a_1 = 0,\ a_2 = 0,\ a_3 = 0,\ a_4 = 1. \tag{8}$$

Then, the Routh-Hurwitz matrix has the following form:

$$\begin{bmatrix} a_4 & a_2 & a_0 \\ a_3 & a_1 & 0 \\ 0 & a_3 & a_1 \end{bmatrix} = \begin{bmatrix} 1 & 0 & 0 \\ 0 & 0 & 0 \\ 0 & 0 & 0 \end{bmatrix}; \tag{9}$$

Accordingly, the main minor determinants are equal:

$$\Delta_1 = a_4 = 1;$$
$$\Delta_2 = \begin{vmatrix} a_4 & a_2 \\ a_3 & a_1 \end{vmatrix} = a_4 \cdot a_1 - a_2 \cdot a_3 = 0;$$
$$\Delta_3 = \begin{vmatrix} a_4 & a_2 & a_0 \\ a_3 & a_1 & 0 \\ 0 & a_3 & a_1 \end{vmatrix} = a_4 \begin{vmatrix} a_1 & 0 \\ a_3 & a_1 \end{vmatrix} - a_2 \begin{vmatrix} a_3 & 0 \\ 0 & a_1 \end{vmatrix} + a_0 \begin{vmatrix} a_3 & a_1 \\ 0 & a_3 \end{vmatrix} = 0. \tag{10}$$

This system is stable since all minor determinants are nonnegative numbers $\Delta_1=1>0$, $\Delta_2=0\geq 0$, and $\Delta_3=0\geq 0$.

Thus, according to the Routh-Hurwitz criterion, the stability hypothesis of the studied differential equations is proved, allowing further analysis of these equations' solutions under different geometrical conditions.

Table 1 shows the layout of the experiment and characteristic parameters (beam length *l*, m; concentrated moment M_0, N·m / distributed load *q*, N/m; Young's modulus *E*, GPa; beam cross-sectional width *b*, m; beam cross-sectional height *h*, m and, accordingly, the moment of inertia of the cross-section *I*, m4) of each.

Table 1. Layout of experiment and characteristic parameters

No. of experiment	1	2	3	4	5
Conditions	Laboratory model	Bridge deflection	Suspended construction	The ceiling beam of a building structure	Flexible stick
l, m	1	20	100	10	2
M_0, N·m / q, N/m	50	5000	10	2000	10
E, GPa	10	200	69	210	1
b, m	0,05	0,5	0,5	0,3	0,01
h, m	0,1	1	0,1	0,6	0,02
I, m^4	4,17e-6	0,0417	1e-6	0,0054	6,67e-9

A hodograph, an amplitude response, and a phase-frequency characteristic were constructed to analyze the solutions of the differential equations for each experiment.

A hodograph is a graphical representation of solutions to differential equations in the complex plane. It allows you to study the influence of system parameters on the stability and dynamic properties of the equation.

The first step in constructing a hodograph is to find the transfer function *G(s)* (s is a complex variable), which is the relation between the input *N(s)* and output *D(s)* functions of the system. For linear differential equations, this can be the Laplace transform. A hodograph is a graph in the complex plane, where the abscissa axis is defined as the axis of the real part of the values *(R)*, and the ordinate axis is the axis of the imaginary part of the values *(I)* of the transfer function. Analysis of the shape and position of the hodograph provides information about the system's stability.

The system is unstable if the hodograph crosses the abscissa axis in the right half-plane. If all points of the hodograph are located in the left half-plane, the system is stable. Thus, a hodograph is a convenient tool for analysing a system's stability and dynamic properties, as well as its response to changes in input data.

The amplitude response illustrates the change in the amplitude of the system's input signal, which depends on its frequency. It is plotted in Cartesian coordinates, where the abscissa axis is the frequency *f* and the ordinate axis is the amplitude of the input signal *A*.

The amplitude response allows us to analyse the gain or attenuation of a signal at different frequency values.

The amplitude-frequency response shows the change in phase of the input signal depending on the change in its frequency.

The amplitude frequency response is a graph in Cartesian coordinates, where the abscissa axis is the frequency *f* and the ordinate axis is the phase of the input signal *p*.

The analysis of the phase-frequency response allows you to detect the delay or advance of the input signal at different frequencies.

A thorough analysis of the amplitude and phase-frequency characteristics of differential equations allows you to assess the system's stability, performance, and accuracy.

The equations and their solutions were analysed using models built in the PyCharm programming environment in the Python programming language.

4 Results

The results of the experiments carried out in this study are illustrated by hodographs and the amplitude and phase-frequency characteristics of the corresponding differential equations.

The graphs of solutions to the equation of deflection of a beam under a concentrated load allow you to model the shape of the deflection of a beam by representing it as a function of coordinates with a certain discreteness along the length of the beam. The curves that illustrate the deflection of a beam have a single point of extremum, which corresponds to the point of load application.

Determining the maximum deflection of a beam is essential for assessing its strength.

The deflection geometry can also be evaluated, as the graphs' shape indicates the beam's deflection type. Comparative analysis of these graphs makes it possible to determine the effect of different values of the moment or geometrical parameters of the beam on the deflection.

Figure 1 shows the graphs of solutions of a beam deflection differential equation under a concentrated load.

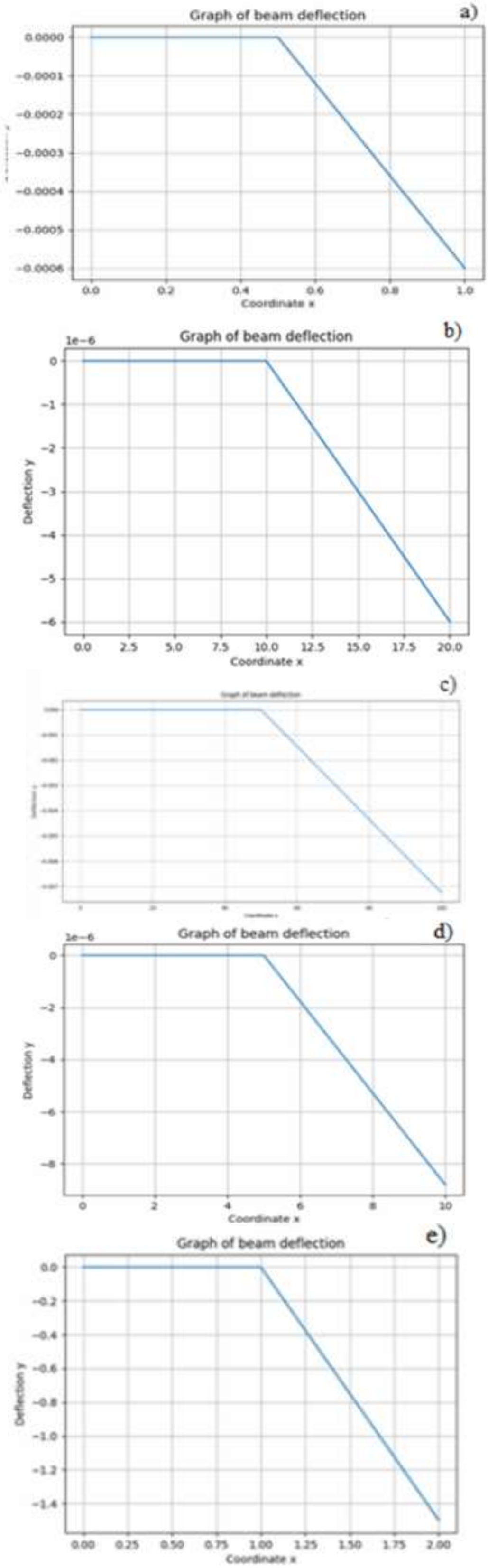

Fig. 1: Graphs of solutions to the differential equation of beam deflection under concentrated load: a - graph of solutions of experiment 1; b - graph of solutions of experiment 2; c - graph of solutions of experiment 3; d - graph of solutions of experiment 4; e - graph of solutions of experiment 5

It is expected that up to the point of application of the concentrated moment M_0, the deflection $v(x)$ is 0. After the point of application of the moment, the deflection graph changes linearly in the negative half-plane, indicating a negative deflection, namely, the concavity of the beam. The deflection value reaches its maximum extreme point at the final coordinate of the beam. The practical value of such a calculation is to make design decisions regarding the optimisation of the beam structure, selection of materials, or reinforcement of beam seats.

Figure 2 shows the graphs of solutions to the differential equation of a beam deflection under a distributed load.

The solutions graph relays the load effect's physical meaning on the beam. In the case of a distributed load, the solution graph of this differential equation has the form of a second-order parabolic curve that is concave downward. This is a typical deflection pattern for a beam under a distributed load. Suppose we take the second-order derivative of the deflection for a coordinate. In that case, the resulting equation includes a term proportional to the square of the distance from a point to each end of the beam, corresponding to a downward concave parabola.

Figure 3 shows hodographs of the beam deflection equation under concentrated load.

The hodograph of Experiment 1 has the shape of an asymmetric arc, as the beam deflection is not the same on both sides of the point where the moment is applied. The intersection with the ordinate axis means that the solution to the equation has a non-zero initial condition, i.e., the beam deflection at the moment's point of application is not zero.

The hodograph of Experiment 2 has an unusual shape. The circle with a curl in the center indicates that the beam deflection is not the same along its length under the action of a point moment. The symmetrical shapes at the ends of the hodograph suggest that the beam has a symmetrical deflection at the ends relative to the point of moment application. This deflection pattern can be caused by the geometry of the beam or the distribution of its internal forces.

The hodograph of Experiment 3 forms concentric circles, a complex phenomenon. Concentric circles indicate beam deflection, which is symmetrical about the center of the coordinates. The loop in the central circle indicates that the beam deflection has a non-zero value at the centre of the coordinates.

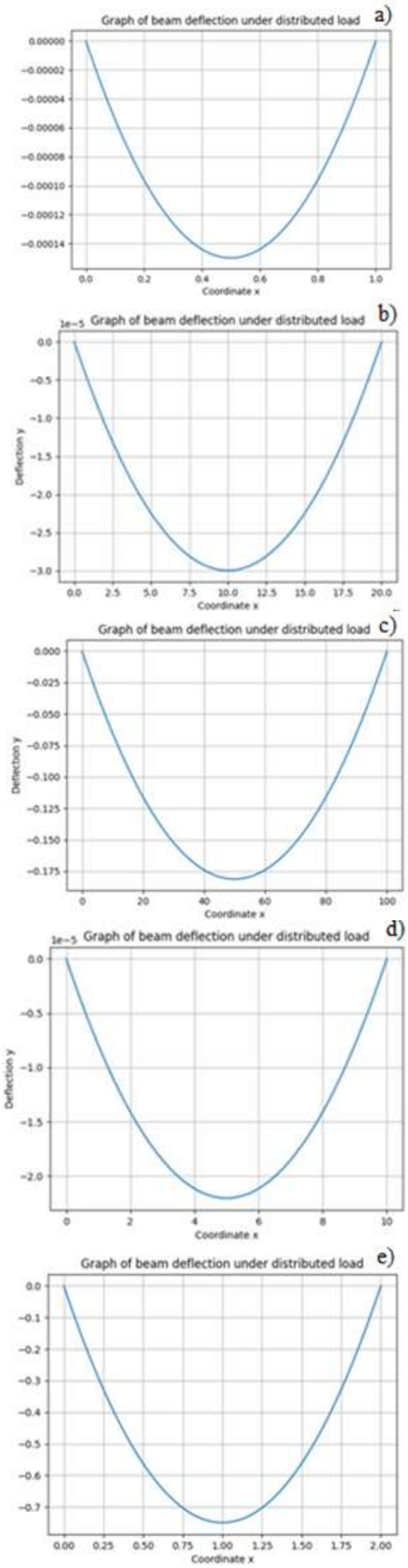

Fig. 2: Graphs of solutions to the differential equation of deflection of a beam under distributed load: a - graph of solutions of experiment 1; b - graph of solutions of experiment 2; c - graph of solutions of experiment 3; d - graph of solutions of experiment 4; e - graph of solutions of experiment 5

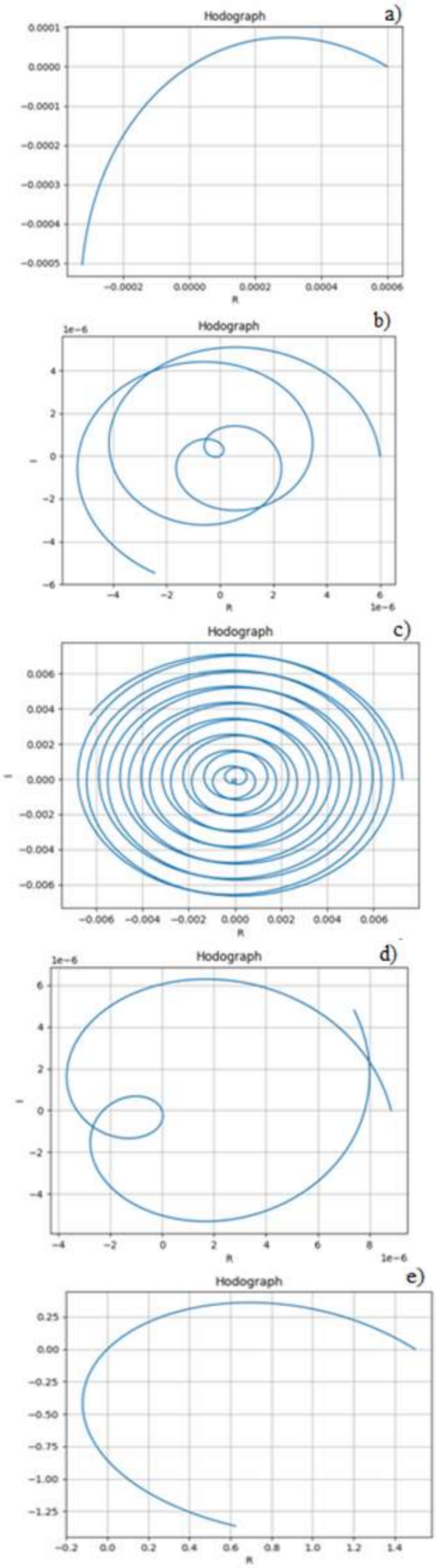

Fig. 3: Hodographs of the differential equation of a beam deflection under concentrated load: a - hodograph of experiment 1; b - hodograph of experiment 2; c - hodograph of experiment 3; d - hodograph of experiment 4; e - hodograph of experiment 5

The hodograph of Experiment 4 forms an asymmetrical circle with a loop on the left-hand side of the coordinates and a crossing of the ends on the right-hand side, which may indicate a complex strain distribution. Such abrupt changes can occur due to sudden changes in load, geometric features of the beam, or fixing conditions.

The hodograph of Experiment 5 has the shape of a half-ellipse. It is almost entirely located in the right part of the coordinates, which may also indicate unusual properties of the strain distribution. Such changes may result from uneven distribution of moments along the beam or other external factors.

The hodographs of the deflection equation of a beam under concentrated load are pretty sensitive to the nature of the load and, in particular, the geometry of the beam. This sensitivity means that even small changes in these parameters significantly affect the system's behaviour, which is reflected in the change in the shape of the hodographs, allowing for better analysis of the deformation and stability of structures.

Figure 4 shows the hodographs of a beam deflection differential equation with a distributed moment.

As seen in Figure 4, the hodograph has the form of a parabola on the left side of the coordinates. This indicates that the beam deflection decreases with increasing distance from the beginning of the beam (usually the left end). This shape of the hodograph shows that the beam is bending in the negative direction from its initial position. In this case, the parabola lying to the left may indicate that the maximum deflection of the beam is located near the left end of the beam. Then, the deflection gradually decreases to zero near the right end of the beam.

The position of the hodograph on the left relative to the ordinate axis confirms the stability of this equation, which has already been announced in the results of the Routh-Hurwitz criterion.

Thus, hodographs represent a system's responses to various inputs in a complex plane. Multiple factors, such as load type, beam geometry, material properties, etc., can determine the hodograph's shape.

The hodograph of the deflection equation of a beam under a distributed load can take the form of a parabola of the features of its solutions related to the load parameters and properties of the beam.

The hodograph of the deflection equation of a beam under a concentrated load can have a more complex shape. Depending on the point of application of the load, the geometry of the beam, and other factors, it may have loops, concentric circles, etc.

Thus, the different shapes of the hodographs of the equations of various types of loading reflect the nature of the system's responses to other types of input signals (i.e., the deflection of the beam under load).

The amplitude and phase-frequency characteristics demonstrate the dynamics of the beam's response to the load applied to it. To assess the system's dynamic stability, it is essential to evaluate the amplitude change with the signal's frequency change. Changes in the phase value allow us to estimate the delay between the change in load value and the signal response.

Figure 5 and Figure 6 show the amplitude and phase-frequency characteristics of the beam deflection equations under concentrated and distributed loading, respectively, for the first experiment.

The downward curve of the amplitude response of the equation of deflection of a beam under a concentrated load (Figure 5) indicates that the beam's amplitude of deflection decreases with increasing load frequency. This can be interpreted as the beam's response to high-frequency loads when the deformation absorption capacity of its material is limited.

The graph of the phase-frequency response (Figure 5) is a straight line with a constant phase value of -1.57 rad, which indicates that the deflection phase lags the load phase. This can be caused by the beam's inertial or damping response to changes in load frequency.

The amplitude characteristic of the deflection equation of a beam with a distributed load (Figure 6) is an increasing curve.

This indicates an increase in the deflection amplitude with an increase in the load frequency. This may be due to the beam's dynamic response to various frequency disturbances, where an increase in frequency provokes an increase in beam deflection.

The phase-frequency characteristic (Figure 6), a straight line with a constant value of 0, indicates that the beam's deflection phase coincides with the load phase. A value of 0 means no delay between the deflection and load phases.

In general, such characteristics can indicate the dynamic behavior of a beam under a distributed load. An increase in amplitude with increasing frequency can indicate significant dynamic effects such as resonance or dynamic amplification.

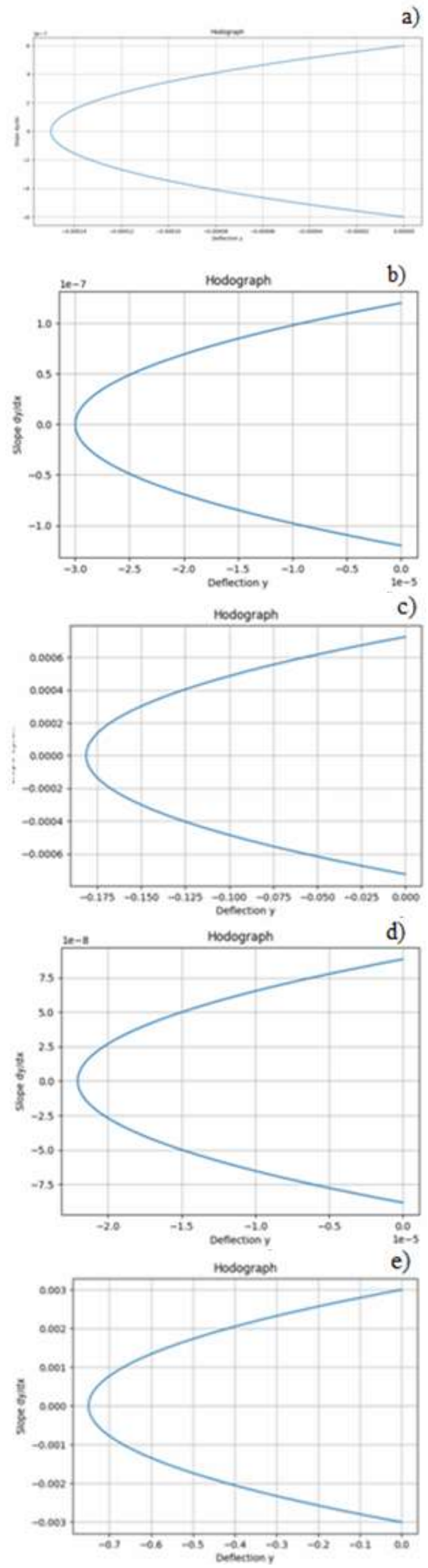

Fig. 4: Hodographs of the beam deflection equation under distributed load: a - hodograph of experiment 1; b - hodograph of experiment 2; c - hodograph of experiment 3; d - hodograph of experiment 4; e - hodograph of experiment 5Step 4: Open your manuscript file, repeat Step 1-3 and copy all styles entitled with HRPUB to your manuscript file.

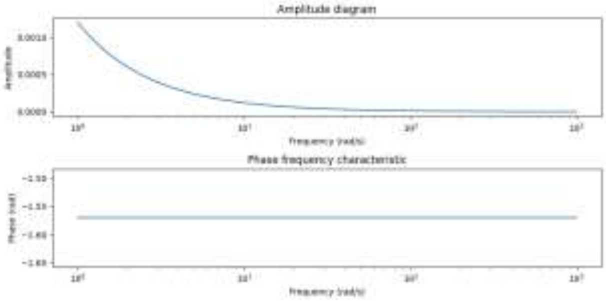

Fig. 5: This is an example of the amplitude diagram and phase-frequency characteristic of the beam deflection equation under concentrated load for the first experiment

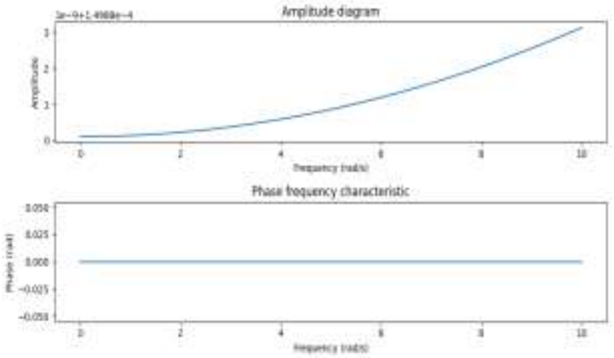

Fig. 6: This is an example of the amplitude and phase-frequency characteristics of the equation of a beam deflection under the action of a distributed load for the first experiment

Phase coherence between deflection and load may indicate efficient energy transfer from the load to the structure.

Since the considered characteristics are typical for each equation, Table 2 and Table 3 in Appendix give the different amplitude values A_N (N is the experiment number) for the beam deflection equations with a concentrated and distributed moment. Each experiment's frequency *f* and phase *p* values are constant. (*f* = const, p = const).

According to the values given in Table 3 (Appendix), the phase and frequency values remain constant. The system's properties do not change with changes in load intensity or beam parameters, at least within the limits of the experiment. Such properties are essential for analyzing system dynamics and stability.

5 Discussion

The analysis of the results obtained in this article shows ways to the practical application of solutions of differential equations, namely, the adoption of design decisions in engineering. It shows how the equations of curves, particularly parabolas, are expressed through physical processes. The conclusion that a differential equation with solutions is stable is proved through the Routh-Hurwitz criterion. The importance of using hodographs as one of the graph-analytical methods to identify the details of the process under study is shown.

Based on the study's results, hodographs are a handy tool for graph-analytical analysis. They provide an understanding of a structure's dynamic properties and resistance to different loads. Using hodographs has made it possible to identify behavioral features of beams that may not always be obvious from other analysis methods. Therefore, this method is of great practical importance for designing and optimizing building structures.

The differential equations for beam deflection under concentrated and distributed loading are stable second-order equations. Their graphs are a simplified representation of the beam, illustrating the distribution of deformations along the length of the beam and allowing the analysis of the physical process under study in various conditions. This study is much more extensive and informative than similar ones, [14]. The paper presents an accurate analytical solution for the static deflection analysis of fully connected composite Timoshenko beams under uniformly distributed and finite loads. It is also worth mentioning the research work [15], where the authors considered the deflection of a cantilever beam. The graph-analytical methods used in this paper have an advantage over modeling based on decomposing functions to the Taylor-Fourier series, as in [16], or over the methods presented in [17]. The approach to analyzing solutions of differential equations would be helpful for further research, [18].

6 Conclusions

This study used second-order differential equations to thoroughly analyze the effects of various loads on building structures, particularly beams. The study's main goal was to improve the understanding of physical processes occurring in structures by mathematical modeling of deformations and graphical and analytical analysis of the obtained solutions.

The Rausch-Hurwitz criterion, used to check the stability of the equations, showed that the systems remain stable under different loading conditions. This confirms the mathematical models' correctness and suitability for practical use in construction.

The graphs of solutions to the deformation equations of beams under concentrated and distributed loads demonstrated characteristic deformation profiles. In particular, the maximum strain occurs at the point of moment application for concentrated loads and has a parabolic shape for distributed loads.

It is appropriate to use hodographs to analyse equation solutions for their dynamic properties. In particular, different forms of hodographs (from parabolas to ellipses) illustrate the peculiarities of systems' behaviour under various loads.

It is shown that a beam's load response depends on the loading frequency, which is an essential aspect in assessing the stability and reliability of structures under different operating conditions.

These methods could be applied in future research to analyse more complex structures such as frames or arches.

An important area for further research is the improvement of numerical methods, such as the finite element method (FEM), to obtain more accurate solutions to differential equations.

In addition, future research should aim to develop structural optimisation methods that minimise deformation and increase the stability and reliability of structures under different types of loading.

Declaration of Generative AI and AI-assisted Technologies in the Writing Process

During the preparation of this work the authors used OpenAI's ChatGPT in order improve readability and language. After using this tool/service, the author reviewed and edited the content as needed and take full responsibility for the content of the publication.

References:

[1] Zwillinger, D., Dobrushkin, V., *Handbook of differential equations*, New York, NY, Chapman and Hall/CRC, 2021. doi: 10.1201/9780429286834.

[2] Belova, M., Denysenko, V., Kartashova, S., Kotlyar, V., Mikhailenko, S., Analysis of the Structure of Chaotic Solutions of Differential Equations, *WSEAS Transactions on Circuits and Systems*, Vol.22, 2023, pp. 75-85. https://doi.org/10.37394/23201.2023.22.10.

[3] Shin, Y., Darbon, J., Karniadakis, G. E., On the convergence of physics informed neural networks for linear second-order elliptic and parabolic type PDEs, *Gllobal Science Press*, Vol.28, No. 5, 2020, pp. 2042-2074. https://doi.org/10.4208/cicp.OA-2020-0193.

[4] Rini, N. W., Saefan, J., Khoiri, N., Lagrangian Equation of Coupled Spring-Pendulum System, *Physics Communication*, Vol.7.1, 2023, pp. 22-27. doi: 10.15294/physcomm.v7i1.40771.

[5] Chakraborty, M., Chakraborty, S., On the consequences of Raychaudhuri equation in Kantowski-Sachs space-time, *Annals of Physics*, Vol.460, 2024, art. 169577. http://dx.doi.org/10.1016/j.aop.2023.169577.

[6] Hassan, T. S., Cesarano, C., El-Nabulsi, R. A., Anukool, W., Improved Hille-type oscillation criteria for second-order quasilinear dynamic equations, *Mathematics*, Vol.10, No.19, 2022, p. 3675. https://doi.org/10.3390/math10193675.

[7] Kumar, S., Ghosh, S., Samet, B., An analysis for heat equations arise in diffusion process using new Yang-Abdel-Aty-Cattani fractional operator, *Mathematical Methods in the Applied Sciences*, Vol.43, No.9, 2020, pp. 6062-6080. doi: 10.1002/mma.6347.

[8] Atangana, A., Akgül, A., Owolabi, K. M., Analysis of fractal fractional differential equations, *Alexandria Engineering Journal*, Vol.59, No.3, 2020, pp. 1117-1134. https://doi.org/10.1016/j.aej.2020.01.005.

[9] Khan, A., Khan, H., Gomez-Aguilar, J.F., Abdeljawad, T., Existence and Hyers-Ulam stability for a nonlinear singular fractional differential equations with Mittag-Leffler kernel, *Chaos, Solitons & Fractals*, Vol.127, 2019, pp. 422-427. https://doi.org/10.1016/j.chaos.2019.07.026.

[10] Benhadri, M., Zeghdoudi, H., Stochastic differential equations and fixed point technique. [Doctoral thesis], Université Frères Mentouri - Constantine 1, 2020, [Online]. https://theses-algerie.com/6227973567361418/these-de-doctorat/universite-freres-mentouri---constantine-1/stochastic-differential-equations-and-fixed-point-technique- (Access Date: 15 July 2024).

[11] Kumar, D., Singh, J., Baleanu, D., On the analysis of vibration equation involving a fractional derivative with Mittag-Leffler law, *Mathematical Methods in the Applied Sciences*, Vol.43, No.1, 2020, pp. 443-457. https://doi.org/10.1002/mma.5903.

[12] Zhang, R.-F., Bilige, S., Bilinear neural network method to obtain the exact analytical solutions of nonlinear partial differential equations and its application to p-gBKP equation, *Nonlinear Dynamics*, Vol.95, 2019,

pp. 3041-3048. doi: 10.1007/s11071-018-04739-z.

[13] Hurwitz, A., Ueber die Bedingungen, unter welchen eine Gleichung nur Wurzeln mit negativen reellen Theilen besitzt, *Mathematische Annalen*, Vol.46, No.2, 1895, pp. 273-284. https://doi.org/10.1007/BF01446812.

[14] Doeva, O., Masjedi, P. K., Weaver, P. M., Static deflection of fully coupled composite Timoshenko beams An exact analytical solution, *European Journal of Mechanics-A/Solids*, Vol.81, 2020, art. 103975. https://doi.org/10.1016/j.euromechsol.2020.103975.

[15] Singhal, D., Narayanamurthy, V., Large and small deflection analysis of a cantilever beam, *Journal of The Institution of Engineers (India): Series A*, Vol.100, No.1, 2019, pp. 83-96. doi: 10.1007/s40030-018-0342-3.

[16] Bai, R., Awtar, S., Chen, G., A closed-form model for nonlinear spatial deflections of rectangular beams in the intermediate range, *International Journal of Mechanical Sciences*, Vol.160, 2019, pp. 229-240. https://doi.org/10.1016/j.ijmecsci.2019.06.042

[17] Jahami, A., Khatib, J. M., Baalbaki, O., Sonebi, M., Prediction of deflection in reinforced concrete beams containing plastic waste, *Academic Journal of Civil Engineering*, Vol.37, No.2, 2019, pp. 551-555. doi: 10.26168/icbbm2019.80.

[18] Atutis, E., Valivonis, J., Atutis, M., Deflection determination method for BFRP prestressed concrete beams under fatigue loading, *Composite Structures*, Vol. 226, 2019, art. 111182. https://doi.org/10.1016/j.compstruct.2019.111182.

Contribution of Individual Authors to the Creation of a Scientific Article (Ghostwriting Policy)

Each author has made an equal contribution.

Sources of Funding for Research Presented in a Scientific Article or Scientific Article Itself

No funding was received for conducting this study.

Conflict of Interest

The authors have no conflicts of interest to declare.

APPENDIX

Table 2. Amplitude, phase, and frequency values for the beam deflection equation with concentrated load

Point number	f, rad/s	p, rad	A_1, m	A_2, m	A_3, m	A_4, m	A_5, m
1	1	-1,5708	0,001199	6,00E-07	0,000145	1,76E-06	1,49925
10	1,873817	-1,5708	0,00064	3,20E-07	7,73E-05	9,41E-07	0,800105
20	3,764936	-1,5708	0,000318	1,59E-07	3,85E-05	4,68E-07	0,398214
30	7,564633	-1,5708	0,000159	7,93E-08	1,92E-05	2,33E-07	0,198192
40	15,19911	-1,5708	7,89E-05	3,94E-08	9,54E-06	1,16E-07	0,098641
50	30,53856	-1,5708	3,93E-05	1,96E-08	4,75E-06	5,78E-08	0,049094
60	61,35907	-1,5708	1,95E-05	9,77E-09	2,36E-06	2,87E-08	0,024434
70	123,2847	-1,5708	9,73E-06	4,86E-09	1,18E-06	1,43E-08	0,012161
80	247,7076	-1,5708	4,84E-06	2,42E-09	5,85E-07	7,12E-09	0,006052
90	497,7024	-1,5708	2,41E-06	1,20E-09	2,91E-07	3,54E-09	0,003012
100	1000	-1,5708	1,20E-06	6,00E-10	1,45E-07	1,76E-09	0,001499

Table 3. Amplitude, phase, and frequency values for the beam deflection equation with a distributed load

Point number	f, rad/s	p, rad	A_1, m	A_2, m	A_3, m	A_4, m	A_5, m
1	0	0	0,00015	3,00E-05	0,181159	2,20E-05	0,749625
10	0,909091	0	0,00015	3,00E-05	0,181343	2,20E-05	0,752775
20	1,919192	0	0,00015	3,00E-05	0,18198	2,20E-05	0,763872
30	2,929293	0	0,00015	3,00E-05	0,183082	2,20E-05	0,783675
40	3,939394	0	0,00015	3,00E-05	0,184666	2,20E-05	0,813554
50	4,949495	0	0,00015	3,00E-05	0,186758	2,20E-05	0,855779
60	5,959596	0	0,00015	3,00E-05	0,189391	2,20E-05	0,913999
70	6,969697	0	0,00015	3,00E-05	0,192609	2,20E-05	0,994157
80	7,979798	0	0,00015	3,00E-05	0,196468	2,20E-05	1,106345
90	8,989899	0	0,00015	3,00E-05	0,201042	2,20E-05	1,268886
100	10	0	0,00015	3,00E-05	0,206419	2,20E-05	1,518544